

## Measurements of Ground-Level Muons at Two Geomagnetic Locations

J. Kremer,<sup>8</sup> M. Boezio,<sup>9</sup> M. L. Ambriola,<sup>1</sup> G. Barbiellini,<sup>11</sup> S. Bartalucci,<sup>4</sup> R. Bellotti,<sup>1</sup> D. Bergström,<sup>9</sup> U. Bravar,<sup>6</sup> F. Cafagna,<sup>1</sup> P. Carlson,<sup>9</sup> M. Casolino,<sup>7</sup> M. Castellano,<sup>1</sup> F. Ciacio,<sup>1</sup> M. Circella,<sup>1</sup> C. De Marzo,<sup>1</sup> M. P. De Pascale,<sup>7</sup> T. Francke,<sup>9</sup> N. Finetti,<sup>7</sup> R. L. Golden,<sup>6,\*</sup> C. Grimani,<sup>12</sup> M. Hof,<sup>8</sup> W. Menn,<sup>8</sup> J. W. Mitchell,<sup>5</sup> A. Morselli,<sup>7</sup> J. F. Ormes,<sup>5</sup> P. Papini,<sup>3</sup> S. Piccardi,<sup>3</sup> P. Picozza,<sup>7</sup> M. Ricci,<sup>4</sup> P. Schiavon,<sup>11</sup> M. Simon,<sup>8</sup> R. Sparvoli,<sup>7</sup> P. Spillantini,<sup>3</sup> S. A. Stephens,<sup>2</sup> S. J. Stochaj,<sup>6</sup> R. E. Streitmatter,<sup>5</sup> M. Suffert,<sup>10</sup> A. Vacchi,<sup>11</sup> N. Weber,<sup>9</sup> and N. Zampa<sup>11</sup>

<sup>1</sup>*Dipartimento di Fisica dell'Università and Sezione INFN di Bari, I-70126 Bari, Italy*

<sup>2</sup>*Tata Institute of Fundamental Research, Bombay 400 005, India*

<sup>3</sup>*Dipartimento di Fisica dell'Università and Sezione INFN di Firenze, I-50125 Firenze, Italy*

<sup>4</sup>*Laboratori Nazionali INFN, I-00044 Frascati, Italy*

<sup>5</sup>*Code 661, NASA/Goddard Space Flight Center, Greenbelt, Maryland 20771*

<sup>6</sup>*Box 3-PAL, New Mexico State University, Las Cruces, New Mexico 88003*

<sup>7</sup>*Dipartimento di Fisica dell'Università and Sezione INFN di Roma, Tor Vergata, I-00133 Roma, Italy*

<sup>8</sup>*Universität Siegen, 57068 Siegen, Germany*

<sup>9</sup>*Royal Institute of Technology (KTH), S-104 05 Stockholm, Sweden*

<sup>10</sup>*Centre des Recherches Nucléaires, BP20, F-67037 Strasbourg-Cedex, France*

<sup>11</sup>*Dipartimento di Fisica dell'Università and Sezione INFN di Trieste, I-34147 Trieste, Italy*

<sup>12</sup>*Dipartimento di Fisica dell'Università di Urbino, I-61029 Urbino, Italy*

(Received 23 July 1999)

We report new measurements of the muon spectra and the muon charge ratio at ground level in the momentum range from 200 MeV/ $c$  to 120 GeV/ $c$  for two different geomagnetic locations. Above 0.9 GeV/ $c$  the absolute spectra measured in the two locations are in good agreement and are about 10% to 15% lower than previous experimental results. At lower momenta the data show latitude dependent geomagnetic effects. These observations are important for the understanding of the observed neutrino anomaly.

PACS numbers: 96.40.Tv, 96.40.Kk, 14.60.Pq

Precise measurements of the muon energy spectrum and charge ratio at sea level over a wide energy range provide information on the propagation of cosmic rays in the atmosphere. Together with data on the primary cosmic rays, muon measurements can be used as a test to check calculations of atmospheric cascades and neutrino fluxes [1]. These latter calculations are used to interpret the recent results on neutrino oscillation from the Super-Kamiokande experiment [2]. Furthermore, spectra of muons at low energies (below a few GeV) measured at different geomagnetic locations are useful to study the effect of Earth's magnetic field on the propagation of the secondary component in the atmosphere [3].

In the past, the muon spectrum has been extensively measured, mainly by solid iron magnet spectrometers in which multiple scattering plays an important role in the momentum resolution, particularly at low energies. Only two measurements have been performed using low mass superconducting magnet spectrometers [4,5]. In this paper we report results from measurements at ground on the muon momentum spectrum and charge ratio from 200 MeV/ $c$  to 120 GeV/ $c$  measured with the NMSU-WIZARD/CAPRICE magnet spectrometer at two different geomagnetic locations. These locations are (i) Lynn Lake, Manitoba, Canada (56.5° N, 101.0° W), at an altitude of 360 m above sea level, and a nominal vertical geomagnetic cutoff of 0.5 GV, and (ii) Fort Sumner, New Mexico,

(34.3° N, 104.1° W), at an altitude of 1270 m and a cutoff of 4.2 GV.

The NMSU-WIZARD/CAPRICE spectrometer was designed as a balloon-borne apparatus for cosmic ray studies. From top to bottom the instrument [6] included a ring imaging Cherenkov (RICH) detector, a time-of-flight (ToF) system, a superconducting magnet spectrometer with a tracking system, and a 7 rad length silicon-tungsten imaging calorimeter. The instruments used in Lynn Lake and Fort Sumner differed in the tracking system and in the radiator material for the RICH. The instrument operated in Lynn Lake during July 1994 (see [7]), hereafter called CAPRICE94, used a stack of multiwire proportional chambers (MWPC), two drift chambers, and a RICH with a solid NaF radiator having a threshold Lorentz factor of 1.5 [8]. The maximum detectable rigidity (MDR) of this spectrometer was 175 GV. During the spring 1997 campaign in Fort Sumner, the MWPCs in the CAPRICE94 apparatus were replaced by an additional drift chamber providing an MDR of 330 GV, and the RICH used a C<sub>4</sub>F<sub>10</sub> gaseous radiator [9] with a threshold Lorentz factor of 20 (hereafter called CAPRICE97 [10]).

About 440 000 and 1200 000 events were recorded at Lynn Lake on the 19th–20th of July 1994 and Fort Sumner between the 26th of April and the 2nd of May 1997, respectively. The precise measurement of the particle trajectory in the tracking system combined with the excellent

performance of the other detectors made it possible to identify muons with negligible background from other particles in the momentum range 0.2–120 GeV/c. At ground, muons are the main component of the cosmic radiation. However, electrons and positrons constitute a small, but detectable, fraction of the muon component at low momenta while the protons amount to a few percent of the muons up to at least 10 GeV/c [11]. Because of the different RICH thresholds, two different muon selection criteria were used to analyze the CAPRICE94 and CAPRICE97 data.

In both experiments, charge one particles moving downward in near vertical direction (the zenith angles were distributed around a mean value of 9 degrees with a maximum of 20 degrees) were selected using the time-of-flight and tracking information. In the CAPRICE94 experiment, muons were above the RICH threshold in the whole energy range of interest. They could be separated from electrons up to about 400 MV and from protons up to 5 GV, above which the Cherenkov angle of protons and muons overlapped [7]. Hence, in this experiment the RICH muon selection was used from 0.2 to 5 GV. Electrons were removed by means of the calorimeter information. Above 300 MV muons could be selected with an efficiency close to 100% and with a negligible electron contamination [12,13]. Above 3 GV  $e^\pm$  amount to less than 0.1% of the muon component [11,12] and, consequently, the calorimeter muon selection was not used above this rigidity. The

surviving proton contamination above 3 GV was calculated by scaling the number of observed particles interacting in the calorimeter by the fraction of interacting protons obtained from data at float where protons dominate (CAPRICE94 was launched on the 8th of August 1994 [7]). This estimated proton background was then subtracted from the positive muon sample.

In the CAPRICE97 experiment the low refractive index of the  $C_4F_{10}$  radiator ( $n = 1.001258$ ) permitted one to extend the rigidity range of the RICH muon selection. Muons started to produce Cherenkov photons in the  $C_4F_{10}$  gas at 2.1 GV and protons at 18.7 GV while electrons were above threshold in the whole rigidity range of interest. Hence, muons were selected requiring Cherenkov light above 2.1 GV and no light below. In this way  $e^\pm$  were rejected up to about 2 GV and protons up to about 20 GV. For larger rigidities the  $e^\pm$  and proton backgrounds were negligible. Furthermore, the proton component was studied up to 20 GeV/c and it was found [14] that the proton to muon ratio decreases from  $(9.7 \pm 0.4)\%$  at 1.1 GeV/c to  $(0.91 \pm 0.09)\%$  at 12.3 GeV/c, compatible with CAPRICE94 and Golden *et al.* results [11]. Below 2 GV, the time-of-flight information was used. The ToF had a resolution of about 230 ps which, with a particle trajectory of about 1.2 m, gave a good rejection of protons against muons for rigidities less than about 1.6 GV. Between 1.6 and 2.1 GV  $\mu^+$  could not be separated from protons and no results on  $\mu^+$  are presented in this rigidity

TABLE I. The  $\mu^-$  and  $\mu^+$  fluxes at ground. Columns 3 and 4 give the  $\mu^+$  and  $\mu^-$  fluxes measured by the CAPRICE94 experiment at an atmospheric depth of 1000 g/cm<sup>2</sup> while columns 5 and 6 are the fluxes measured by CAPRICE97 at 886 g/cm<sup>2</sup>. The errors include both statistical and systematic errors.

Momentum interval GeV/c	Mean momentum GeV/c	CAPRICE94 (GeV/c m <sup>2</sup> sr s) <sup>-1</sup>		CAPRICE97 (GeV/c m <sup>2</sup> sr s) <sup>-1</sup>	
		$\mu^+$	$\mu^-$	$\mu^+$	$\mu^-$
0.2–0.3	0.25	$(1.4 \pm 0.2) \times 10^1$	$(1.1 \pm 0.1) \times 10^1$	$(1.2 \pm 0.1) \times 10^1$	$(1.07 \pm 0.09) \times 10^1$
0.3–0.4	0.35	$(1.68 \pm 0.08) \times 10^1$	$(1.36 \pm 0.07) \times 10^1$	$(1.70 \pm 0.08) \times 10^1$	$(1.52 \pm 0.07) \times 10^1$
0.40–0.55	0.47	$(1.72 \pm 0.05) \times 10^1$	$(1.44 \pm 0.04) \times 10^1$	$(2.03 \pm 0.06) \times 10^1$	$(1.79 \pm 0.05) \times 10^1$
0.55–0.70	0.62	$(1.66 \pm 0.04) \times 10^1$	$(1.35 \pm 0.03) \times 10^1$	$(2.12 \pm 0.06) \times 10^1$	$(1.86 \pm 0.05) \times 10^1$
0.70–0.85	0.78	$(1.56 \pm 0.04) \times 10^1$	$(1.33 \pm 0.03) \times 10^1$	$(2.04 \pm 0.05) \times 10^1$	$(1.76 \pm 0.05) \times 10^1$
0.85–1.0	0.92	$(1.48 \pm 0.03) \times 10^1$	$(1.21 \pm 0.03) \times 10^1$	$(1.92 \pm 0.05) \times 10^1$	$(1.64 \pm 0.04) \times 10^1$
1.0–1.2	1.1	$(1.30 \pm 0.03) \times 10^1$	$(1.10 \pm 0.03) \times 10^1$	$(1.77 \pm 0.04) \times 10^1$	$(1.48 \pm 0.03) \times 10^1$
1.2–1.4	1.3	$(1.20 \pm 0.03) \times 10^1$	$(1.01 \pm 0.02) \times 10^1$	$(1.55 \pm 0.03) \times 10^1$	$(1.28 \pm 0.03) \times 10^1$
1.4–1.6	1.5	$10.2 \pm 0.2$	$8.7 \pm 0.2$	$13.9 \pm 0.3$	$11.40 \pm 0.26$
1.6–2.1	1.84	$9.1 \pm 0.2$	$7.3 \pm 0.1$		$9.2 \pm 0.19$
2.1–2.94	2.49	$6.6 \pm 0.1$	$5.20 \pm 0.09$	$7.0 \pm 0.9$	$5.7 \pm 0.7$
2.94–4.12	3.49	$4.12 \pm 0.07$	$3.38 \pm 0.06$	$4.8 \pm 0.1$	$3.86 \pm 0.08$
4.12–5.5	4.78	$2.53 \pm 0.05$	$1.98 \pm 0.04$	$2.94 \pm 0.06$	$2.31 \pm 0.05$
5.5–7.0	6.21	$1.61 \pm 0.03$	$1.25 \pm 0.03$	$1.78 \pm 0.04$	$1.37 \pm 0.03$
7.0–10.0	8.37	$(9.0 \pm 0.2) \times 10^{-1}$	$(6.9 \pm 0.1) \times 10^{-1}$	$(10.2 \pm 0.2) \times 10^{-1}$	$(7.8 \pm 0.2) \times 10^{-1}$
10.0–15.5	12.42	$(3.89 \pm 0.08) \times 10^{-1}$	$(3.09 \pm 0.07) \times 10^{-1}$	$(4.14 \pm 0.09) \times 10^{-1}$	$(3.20 \pm 0.07) \times 10^{-1}$
15.5–23.0	18.85	$(1.38 \pm 0.04) \times 10^{-1}$	$(1.08 \pm 0.03) \times 10^{-1}$	$(1.54 \pm 0.04) \times 10^{-1}$	$(1.16 \pm 0.03) \times 10^{-1}$
23.0–31.1	26.68	$(6.3 \pm 0.3) \times 10^{-2}$	$(4.6 \pm 0.2) \times 10^{-2}$	$(6.4 \pm 0.2) \times 10^{-2}$	$(4.5 \pm 0.2) \times 10^{-2}$
31.1–43.6	36.69	$(2.8 \pm 0.1) \times 10^{-2}$	$(1.9 \pm 0.1) \times 10^{-2}$	$(2.8 \pm 0.1) \times 10^{-2}$	$(2.03 \pm 0.08) \times 10^{-2}$
43.6–61.1	51.47	$(9.9 \pm 0.7) \times 10^{-3}$	$(7.1 \pm 0.6) \times 10^{-3}$	$(10.2 \pm 0.5) \times 10^{-3}$	$(7.7 \pm 0.4) \times 10^{-3}$
61.1–85.6	72.08	$(3.6 \pm 0.3) \times 10^{-3}$	$(3.0 \pm 0.3) \times 10^{-3}$	$(4.2 \pm 0.3) \times 10^{-3}$	$(3.2 \pm 0.2) \times 10^{-3}$
85.6–120.0	100.96	$(1.4 \pm 0.2) \times 10^{-3}$	$(1.2 \pm 0.2) \times 10^{-3}$	$(1.5 \pm 0.1) \times 10^{-3}$	$(1.1 \pm 0.1) \times 10^{-3}$

interval. Because of the good  $e^\pm$  rejection by the RICH selection in the low energy range, the calorimeter was not used to select muons in the CAPRICE97 analysis.

The absolute particle fluxes were calculated from the number of observed muons taking into account the geometrical factor, spectrometer live time, and selection efficiencies. The geometrical factor, determined with simulation techniques [15], was found to vary with rigidity. It increased from  $145 \text{ cm}^2 \text{ sr}$  at  $0.25 \text{ GV}$  to  $180 \text{ cm}^2 \text{ sr}$  for  $\mu^-$  at  $1 \text{ GV}$  and from  $139 \text{ cm}^2 \text{ sr}$  at  $0.25 \text{ GV}$  to  $180 \text{ cm}^2 \text{ sr}$  at  $1 \text{ GV}$  for  $\mu^+$  in CAPRICE94, and from  $122 \text{ cm}^2 \text{ sr}$  at  $0.25 \text{ GV}$  to  $173 \text{ cm}^2 \text{ sr}$  at  $1 \text{ GV}$  for  $\mu^-$  and from  $110 \text{ cm}^2 \text{ sr}$  at  $0.25 \text{ GV}$  to  $173 \text{ cm}^2 \text{ sr}$  at  $1 \text{ GV}$  for  $\mu^+$  in CAPRICE97. The geometrical factor was checked by two other methods and they all agree within 2% above  $0.5 \text{ GV}$  and within 5% below  $0.5 \text{ GV}$  [7]. On the above calculations it was assumed that there is no variation of the muon intensity over the acceptance angle. The effect on the geometrical factor due to the intensity variation was examined using the measured muon spectra [16] and the observed zenithal distribution in our apparatus in the rigidity range  $0.2$  to  $1.5 \text{ GV}$ . We found that the calculated geometrical factor would be reduced by about 3%. We have not included this uncertainty in the estimation of the flux due to the dependence on the energy of this effect.

The efficiency of each detector was carefully determined by selecting a sample of muons with the remaining detectors [7,12,14]. The agreements found between CAPRICE94 results and those from other experiments for several different particle spectra (e.g., [7] for protons and helium nuclei) give us confidence in our procedures.

The observed muon fluxes are presented in Table I. The mean values are obtained following the method described in [17] using the spectral shape of the Allkofer *et al.* best fit [18]. The CAPRICE94 measurements were taken at an atmospheric depth of  $1000 \text{ g/cm}^2$  and the CAPRICE97 data at  $886 \text{ g/cm}^2$ . The CAPRICE94 fluxes were extrapolated to CAPRICE97 atmospheric depth by scaling the fluxes with an exponential attenuation where the attenuation length was derived from the CAPRICE94 ascent muon data [12,13] (the scaling factor decreases nearly exponentially from 1.5 at  $0.2 \text{ GeV}/c$  to less than 1.1 at  $7 \text{ GeV}/c$  and becomes 1 above  $50 \text{ GeV}/c$ ). This procedure may contribute to the uncertainty of the flux normalization to a maximum of a few percent. The resulting muon spectra at ground (multiplied by  $p^2$ , where  $p$  is the momentum in  $\text{GeV}/c$ ) are shown in Figs. 1(a) and 1(b). Above  $1 \text{ GeV}/c$  there is an excellent agreement, within 3%, between CAPRICE97 data and the CAPRICE94 data extrapolated to  $886 \text{ g/cm}^2$ . Below  $1 \text{ GeV}/c$ , the CAPRICE97 negative and positive muon spectra are significantly lower than the CAPRICE94 results. The difference increases with decreasing momentum and this suggests a latitude dependent geomagnetic effect. Furthermore, the effect on the  $\mu^+$  spectrum is comparatively stronger than on the  $\mu^-$  which can be clearly seen in the

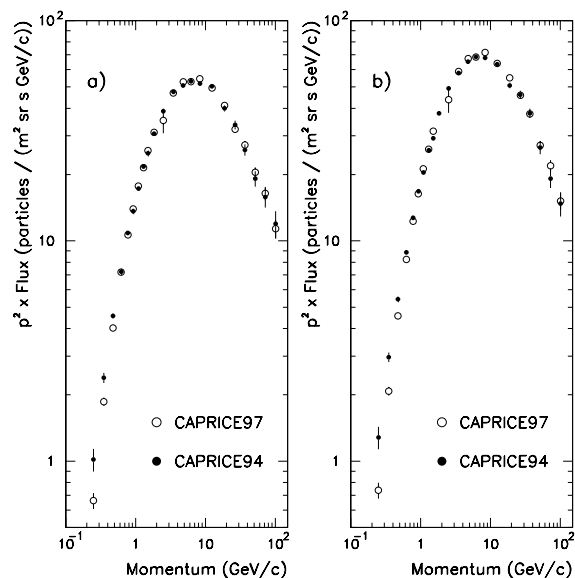


FIG. 1. The observed flux multiplied by the momentum squared at ground level ( $886 \text{ g/cm}^2$  residual atmosphere) as a function of momentum for (a)  $\mu^-$  and (b)  $\mu^+$ . The CAPRICE94 data have been extrapolated to the atmospheric depth of  $886 \text{ g/cm}^2$  scaling the fluxes with an exponential attenuation length which was experimentally determined from the CAPRICE94 ascent muon data [12,13].

muon charge ratio and this has the advantage of being independent of the atmospheric extrapolation of the spectra. Figure 2 shows the charge ratio as a function of momentum obtained with CAPRICE94 and CAPRICE97. An excellent agreement is found between the measurements above  $1 \text{ GeV}/c$ . Below this momentum the CAPRICE97 charge ratio decreases while the CAPRICE94 ratio remains constant. The mean value of the charge ratio between

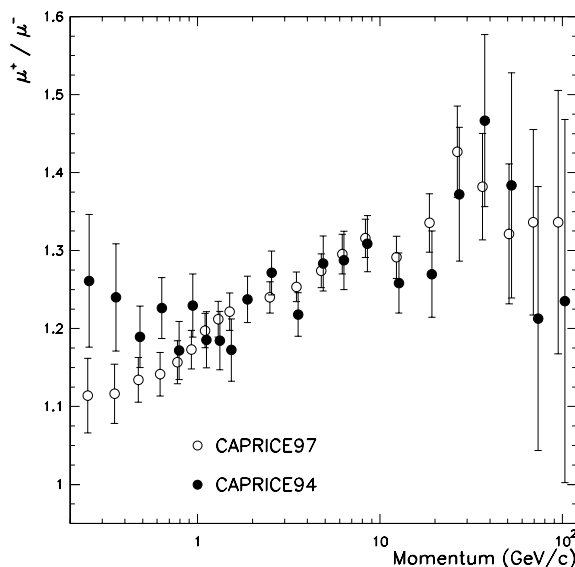


FIG. 2. The muon charge ratio as a function of momentum measured by CAPRICE94 and CAPRICE97. The abscissae of the CAPRICE94 data points have been slightly displaced.

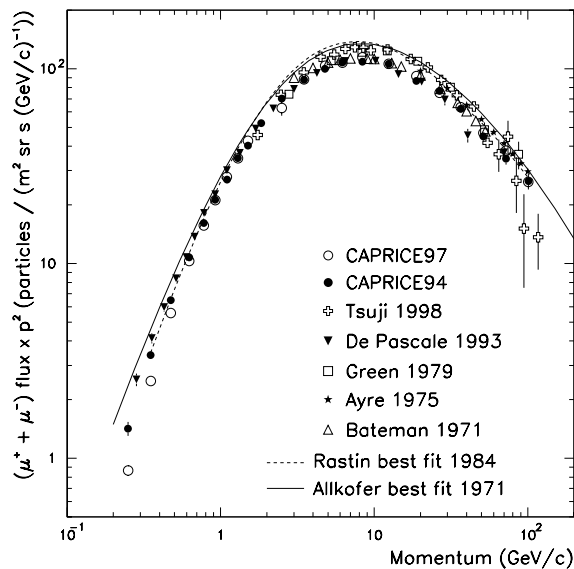


FIG. 3. The  $(\mu^+ + \mu^-)$  spectrum at sea level measured by CAPRICE94 and CAPRICE97, and other experiments [5,16,19–21]. The lines refer to best fits of experimental data not shown here. The fluxes are multiplied by  $p^2$ , where  $p$  is the momentum in  $\text{GeV}/c$ .

0.2 and 0.55  $\text{GeV}/c$  is  $1.12 \pm 0.02$  for CAPRICE97 and  $1.21 \pm 0.03$  for CAPRICE94.

Figure 3 shows the total muon fluxes  $(\mu^+ + \mu^-)$  multiplied by  $p^2$  extrapolated to sea level together with other measurements and the best fits of experimental data (all data extrapolated to sea level). An excellent agreement is also found with the muon data obtained by the MASS89 experiment [5] which used a similar configuration of the same superconducting magnet but with different detectors. The differences with the older measurements, mainly obtained using solid iron magnetic spectrometers, are up to 20%. One should note that a 10% error in momentum implies a 20% error in flux times  $p^2$ . Some data differ also in shape [19,22] with our measurements.

It is important to point out the difference in the intensity of the differential spectrum between our results and the best fit of the experimental data of Allkofer *et al.* [18] which have been frequently used as reference measurements. For example, our flux values extrapolated to sea level at 1  $\text{GeV}/c$  are  $23.7 \pm 0.3$  for CAPRICE94 and  $24.0 \pm 0.3$   $(\text{m}^2 \text{sr s GeV}/c)^{-1}$  for CAPRICE97. This is 14% lower than the value of  $27.9$   $(\text{m}^2 \text{sr s GeV}/c)^{-1}$  in [18] but in agreement with the old value of  $24$   $(\text{m}^2 \text{sr s GeV}/c)^{-1}$  given by Rossi in 1948 [23]. It is worthy to point out that the momentum measurements in the early experiments could have uncertainties due to scattering in the magnet especially at small momenta.

In conclusion, we have presented two new measurements of the muon spectra and charge ratio over three decades in momentum taken at ground level at two different geomagnetic locations. Above 1  $\text{GeV}/c$  the two mea-

sured spectra agree with each other within about 3%. For momenta below 1  $\text{GeV}/c$  our data suggest a geomagnetic effect both in the spectra and in the charge ratio. The relevance of geomagnetic effects to the neutrino calculations have been investigated by [24].

\*Deceased.

- [1] M. Honda *et al.*, Phys. Lett. B **248**, 193 (1990); M. Honda *et al.*, Phys. Rev. D **52**, 4985 (1995); G. Barr, T.K. Gaisser, and T. Stanev, Phys. Rev. D **39**, 3532 (1989); T.K. Gaisser and T. Stanev, in *Proceedings of the 24th International Cosmic Ray Conference, Rome* (Arti Grafiche Editoriali, Urbino, Italy, 1995), Vol. 1, p. 694; E.V. Bugaev and V.A. Naumov, Phys. Lett. B **232**, 391 (1989).
- [2] Y. Fukuda *et al.*, Phys. Rev. Lett. **81**, 1562 (1998).
- [3] S.A. Stephens, in *Proceedings of the 16th International Cosmic Ray Conference, Kyoto* (Institute for Cosmic Ray Research, Tokyo, 1979), Vol. 10, p. 90.
- [4] S.A. Stephens and R. Golden, in *Proceedings of the 20th International Cosmic Ray Conference, Moscow* (NAUKA, Moscow, 1987), Vol. 6, p. 173.
- [5] M.P. De Pascale *et al.*, J. Geophys. Res. **98**, 3501 (1993).
- [6] R. Golden *et al.*, Nucl. Instrum. Methods Phys. Res., Sect. A **306**, 366 (1991); M. Hof *et al.*, Nucl. Instrum. Methods Phys. Res., Sect. A **345**, 561 (1994); M. Bocciolini *et al.*, Nucl. Instrum. Methods Phys. Res., Sect. A **370**, 403 (1996).
- [7] M. Boezio *et al.*, Astrophys. J. **518**, 457 (1999).
- [8] P. Carlson *et al.*, Nucl. Instrum. Methods Phys. Res., Sect. A **349**, 577 (1994); G. Barbiellini *et al.*, Nucl. Instrum. Methods Phys. Res., Sect. A **371**, 169 (1996).
- [9] G. Barbiellini *et al.*, in *Proceedings of the 25th International Cosmic Ray Conference, Durban, South Africa* (Potchefstroomse Universiteit, Potchefstroomse, South Africa, 1997), Vol. 5, p. 1; T. Francke *et al.*, Nucl. Instrum. Methods Phys. Res., Sect. A **433**, 87 (1999).
- [10] M.L. Ambriola *et al.*, Nucl. Phys. B (Proc. Suppl.) **78**, 32 (1999).
- [11] R.L. Golden *et al.*, J. Geophys. Res. **100**, 515 (1995).
- [12] M. Boezio, Ph.D. thesis, Royal Institute of Technology, Stockholm, 1998; [http://msia02.msi.se/group\\_docs/astro/research/CAPRICE.html](http://msia02.msi.se/group_docs/astro/research/CAPRICE.html)
- [13] M. Boezio *et al.*, Phys. Rev. Lett. **82**, 4757 (1999).
- [14] J. Kremer, Ph.D. thesis, Universität-Gesamthochschule-Siegen, Siegen, Germany, 1999.
- [15] J.D. Sullivan, Nucl. Instrum. Methods Phys. Res., Sect. A **95**, 5 (1971).
- [16] S. Tsuji *et al.*, J. Phys. G **24**, 1805 (1998).
- [17] G.D. Lafferty and T.T. Wyatt, Nucl. Instrum. Methods Phys. Res., Sect. A **355**, 541 (1995).
- [18] O.C. Allkofer *et al.*, Phys. Lett. **36B**, 425 (1971).
- [19] P.J. Green *et al.*, Phys. Rev. D **20**, 1598 (1979).
- [20] C.A. Ayre *et al.*, J. Phys. G **1**, 584 (1975).
- [21] B.J. Bateman *et al.*, Phys. Lett. **36B**, 144 (1971).
- [22] B.C. Rastin, J. Phys. G **10**, 1609 (1984).
- [23] B. Rossi, Rev. Mod. Phys. **20**, 537 (1948).
- [24] P. Lipari, T. Stanev, and T.K. Gaisser, Phys. Rev. D **58**, 73003 (1998).